On the precision of a data-driven estimate of the pseudoscalar-pole contribution to hadronic light-by-light scattering in the muon $g-2$

Andreas Nyffeler

Institute for Nuclear Physics
Johannes Gutenberg Universität Mainz, Germany
nyffeler@kph.uni-mainz.de

Flavour changing and conserving processes 2015
Capri island, Italy
September 10, 2015

JOHANNES GUTENBERG UNIVERSITÄT MAINZ

SFB 1044
THE LOW-ENERGY FRONTIER OF THE STANDARD MODEL

Outline

- Introduction
- Pion-pole contribution
  - 3-dim. integral representation, model independent weight functions
  - Contributions to $a_\mu^{\mathrm{HLbL};\pi^0}$ from different momentum regions
  - Impact of form factor uncertainties on $a_\mu^{\mathrm{HLbL};\pi^0}$
- Pole contributions from η and η'
  - Weight functions
  - Contributions from different momentum regions
  - Impact of form factor uncertainties
- Conclusions and Outlook

Muon $g-2$: current status

Contribution	$a_\mu \times 10^{11}$	Reference
QED (leptons)	116 584 718.853 $\pm$ 0.036	Aoyama et al. '12
Electroweak	153.6 $\pm$ 1.0	Gnendiger et al. '13
HVP: LO	6907.5 $\pm$ 47.2	Jegerlehner, Szafron '11
NLO	-100.3 $\pm$ 2.2	Jegerlehner, Szafron '11
NNLO	12.4 $\pm$ 0.1	Kurz et al. '14
HLbL	116 $\pm$ 40	Jegerlehner, AN '09
NLO	3 $\pm$ 2	Colangelo et al. '14
Theory (SM)	116 591 811 $\pm$ 62	
Experiment	116 592 089 $\pm$ 63	Bennett et al. '06
Experiment - Theory	278 $\pm$ 88	3.1 σ

HVP: Hadronic vacuum polarization

HLbL: Hadronic light-by-light scattering

Other estimate: $a_\mu^{\mathrm{HLbL}} = (105 \pm 26) \times 10^{-11}$ (Prades, de Rafael, Vainshtein '09).

Discrepancy a sign of New Physics ? Hadronic uncertainties need to be better controlled in order to fully profit from future $g-2$ experiments with $\delta a_\mu = 16 \times 10^{-11}$. Way forward for HVP seems clear with more precise measurements for $\sigma(e^+e^- \to \text{hadrons})$, not so obvious how to improve HLbL.

HLbL in muon $g-2$

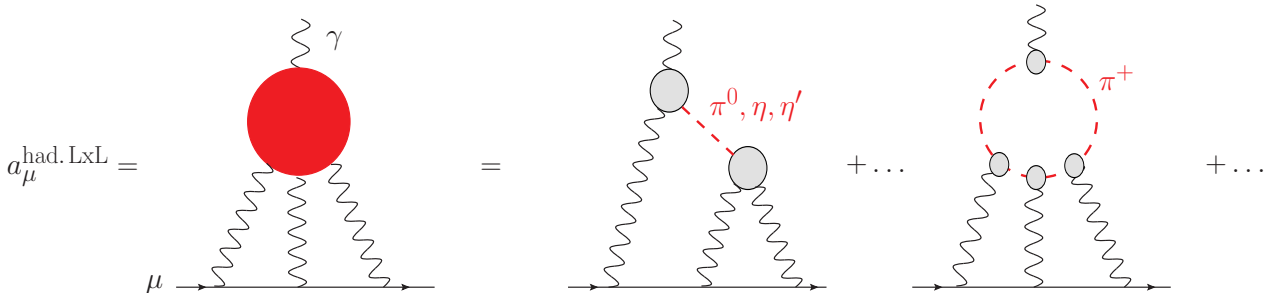

- Only model calculations so far: large uncertainties, difficult to control.
- Frequently used estimates:

  $a_\mu^{\text{HLbL}} = (105 \pm 26) \times 10^{-11}$ (Prades, de Rafael, Vainshtein '09)

  $a_\mu^{\text{HLbL}} = (116 \pm 40) \times 10^{-11}$ (AN '09; Jegerlehner, AN '09)

  Based almost on same input: calculations by various groups using different models for individual contributions. Error estimates are mostly guesses !
- Need much better understanding of complicated hadronic dynamics to get reliable error estimate of $\pm 20 \times 10^{-11}$ ($\sim 20\%$) (or even 10%).
- Recent new proposal: Colangelo et al. '14, '15; Pauk, Vanderhaeghen '14: use dispersion relations (DR) to connect contribution to HLbL from light pseudoscalars to in principle measurable form factors and cross-sections:

  $$\gamma^*\gamma^* \rightarrow \pi^0, \eta, \eta'$$
  $$\gamma^*\gamma^* \rightarrow \pi\pi$$

  Could connect HLbL uncertainty to exp. measurement errors, like HVP.
- Maybe in future: HLbL from Lattice QCD. First steps: Blum et al. '05, ..., '14, '15. Work started by Mainz group.

Pseudoscalar contribution to HLbL

- Most calculations for neutral pion and all light pseudoscalars π^0, η, η' agree at level of 15%, but full range of estimates is much larger:

$$a_\mu^{\mathrm{HLbL};\pi^0} = (50-80)\times 10^{-11} = (65\pm 15)\times 10^{-11}\ (\pm 23\%)$$
$$a_\mu^{\mathrm{HLbL};\mathrm{P}} = (59-114)\times 10^{-11} = (87\pm 27)\times 10^{-11}\ (\pm 31\%)$$

  Note: not always clear, what is calculated, e.g. for π^0: pion-pole (as in DR approach), pion-pole with constant form factor at external vertex (Melnikov, Vainshtein '04), pion-exchange with off-shell form factors.

- This talk: try to study precision which could be reached with a data-driven estimate of the pseudoscalar-pole contribution to HLbL.
- Show relevant momentum regions where data on doubly off-shell form factor $\mathcal{F}_{\pi^0\gamma^*\gamma^*}(-Q_1^2,-Q_2^2)$ will be needed from direct experimental measurements, via a DR for form factor itself (Hoferichter et al. '14) or from Lattice QCD to better control this numerically dominant contribution to HLbL and its uncertainty.
- Present impact on precision of $a_\mu^{\mathrm{HLbL;P}}$ based on estimated experimental uncertainties of $\mathcal{F}_{\pi^0\gamma^*\gamma^*}(-Q_1^2,-Q_2^2)$ using results from Monte Carlo simulation for BES III (Mainz group: Denig, Redmer, Wasser).
- Similar to "pie-charts" for a_μ^{HVP} and its uncertainty $\delta a_\mu^{\mathrm{HVP}}$ as function of centre-of-mass energy $\sqrt{s}$.

Pion-pole contribution (Knecht, AN '02)

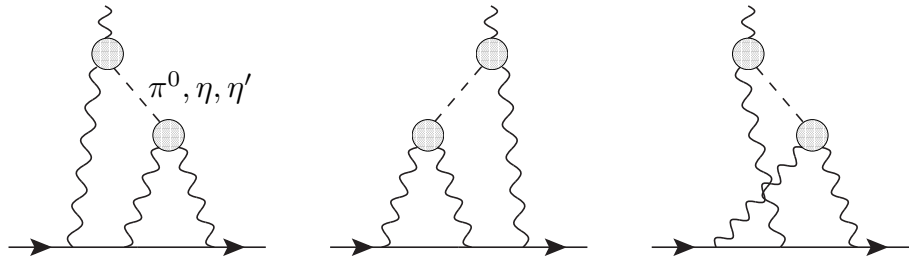

$$a_\mu^{\mathrm{HLbL};\pi^0} = \left(\frac{\alpha}{\pi}\right)^3 \left[a_\mu^{\mathrm{HLbL};\pi^0(1)} + a_\mu^{\mathrm{HLbL};\pi^0(2)}\right]$$

$$a_\mu^{\mathrm{HLbL};\pi^0(1)} = \int \frac{d^4q_1}{(2\pi)^4}\frac{d^4q_2}{(2\pi)^4} \frac{1}{q_1^2 q_2^2 (q_1+q_2)^2[(p+q_1)^2 - m_\mu^2][(p-q_2)^2 - m_\mu^2]} \times \frac{\mathcal{F}_{\pi^0\gamma^*\gamma^*}(q_1^2,(q_1+q_2)^2)\ \mathcal{F}_{\pi^0\gamma^*\gamma^*}(q_2^2,0)}{q_2^2 - m_\pi^2}\ \tilde{T}_1(q_1,q_2;p)$$

$$a_\mu^{\mathrm{HLbL};\pi^0(2)} = \int \frac{d^4q_1}{(2\pi)^4}\frac{d^4q_2}{(2\pi)^4} \frac{1}{q_1^2 q_2^2 (q_1+q_2)^2[(p+q_1)^2 - m_\mu^2][(p-q_2)^2 - m_\mu^2]} \times \frac{\mathcal{F}_{\pi^0\gamma^*\gamma^*}(q_1^2,q_2^2)\ \mathcal{F}_{\pi^0\gamma^*\gamma^*}((q_1+q_2)^2,0)}{(q_1+q_2)^2 - m_\pi^2}\ \tilde{T}_2(q_1,q_2;p)$$

where $p^2 = m_\mu^2$ and the external photon has now zero four-momentum (soft photon).

Pion-pole contribution determined by measurable pion transition form factor $\mathcal{F}_{\pi^0\gamma^*\gamma^*}(q_1^2, q_2^2)$ (on-shell pion, one or two off-shell photons). Currently, only single-virtual TFF $\mathcal{F}_{\pi^0\gamma^*\gamma^*}(-q^2, 0)$ has been measured by CELLO, CLEO, BABAR, Belle (mostly) for spacelike momenta. Analysis ongoing at BES III, measurement planned at KLOE-2. Measurement of double-virtual form factor planned at BES III. Analogously for η, η'-pole contributions.

3-dimensional integral representation (Jegerlehner, AN '09)

$$a_\mu^{\mathrm{HLbL};\pi^0} = \left(\frac{\alpha}{\pi}\right)^3 \left[a_\mu^{\mathrm{HLbL};\pi^0(1)} + a_\mu^{\mathrm{HLbL};\pi^0(2)}\right]$$

$$a_\mu^{\mathrm{HLbL};\pi^0(1)} = \int_0^\infty dQ_1 \int_0^\infty dQ_2 \int_{-1}^1 dt\, w_1(Q_1, Q_2, t) \mathcal{F}_{\pi^0\gamma^*\gamma^*}(-Q_1^2, -(Q_1+Q_2)^2) \mathcal{F}_{\pi^0\gamma^*\gamma^*}(-Q_2^2, 0)$$

$$a_\mu^{\mathrm{HLbL};\pi^0(2)} = \int_0^\infty dQ_1 \int_0^\infty dQ_2 \int_{-1}^1 dt\, w_2(Q_1, Q_2, t) \mathcal{F}_{\pi^0\gamma^*\gamma^*}(-Q_1^2, -Q_2^2) \mathcal{F}_{\pi^0\gamma^*\gamma^*}(-(Q_1+Q_2)^2, 0)$$

$$w_1(Q_1, Q_2, t) = \left(-\frac{2\pi}{3}\right) \sqrt{1-t^2}\, \frac{Q_1^3 Q_2^3}{Q_2^2 + m_\pi^2}\, I_1(Q_1, Q_2, t)$$

$$w_2(Q_1, Q_2, t) = \left(-\frac{2\pi}{3}\right) \sqrt{1-t^2}\, \frac{Q_1^3 Q_2^3}{(Q_1+Q_2)^2 + m_\pi^2}\, I_2(Q_1, Q_2, t)$$

- After Wick rotation: Q_1, Q_2 are Euclidean (spacelike) four-momenta. Integrals run over the lengths of the four-vectors with $Q_i \equiv |(Q_i)_\mu|, i = 1, 2$ and angle θ between them: $Q_1 \cdot Q_2 = Q_1 Q_2 \cos\theta$, $t = \cos\theta$.
- Separation of generic kinematics described by model-independent weight functions $w_{1,2}(Q_1, Q_2, t)$ and double-virtual form factors $\mathcal{F}_{\pi^0\gamma^*\gamma^*}(-Q_1^2, -Q_2^2)$ which can in principle be measured.
- $w_{1,2}(Q_1, Q_2, t)$: dimensionless. $w_2(Q_1, Q_2, t)$ symmetric under $Q_1 \leftrightarrow Q_2$.
- $w_{1,2}(Q_1, Q_2, t) \to 0$ for $Q_{1,2} \to 0$. $w_{1,2}(Q_1, Q_2, t) \to 0$ for $t \to \pm 1$.

Relevant momentum regions in $a_\mu^{\mathrm{HLbL};\pi^0}$

Weight function $w_1(Q_1, Q_2, t)$

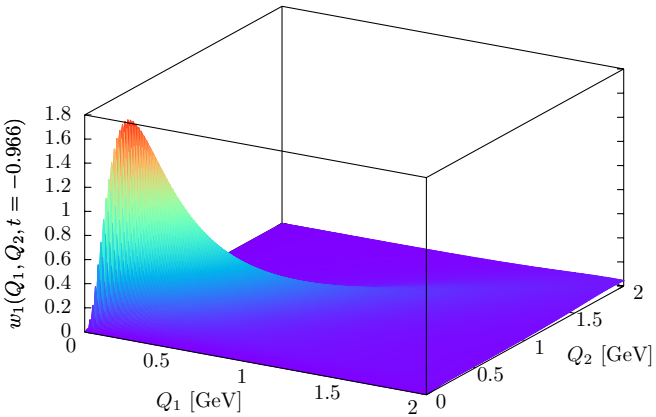

$t = -0.966, \quad \theta = 165°$

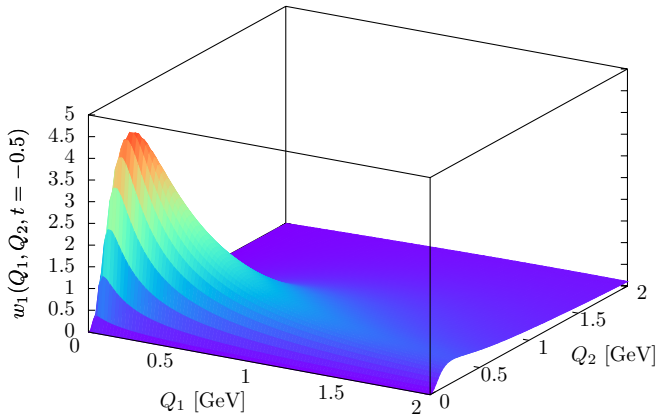

$t = -0.5, \quad \theta = 120°$

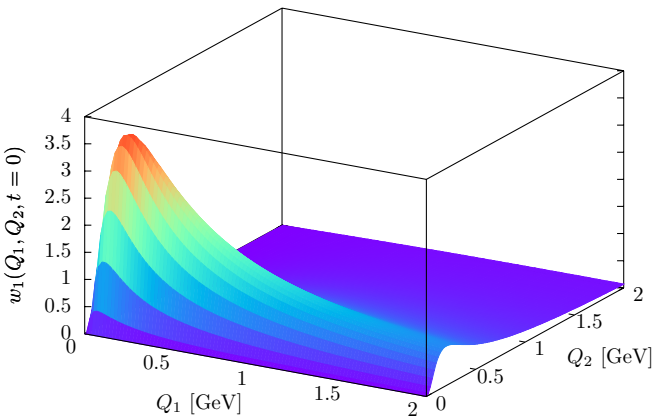

$t = 0, \quad \theta = 90°$

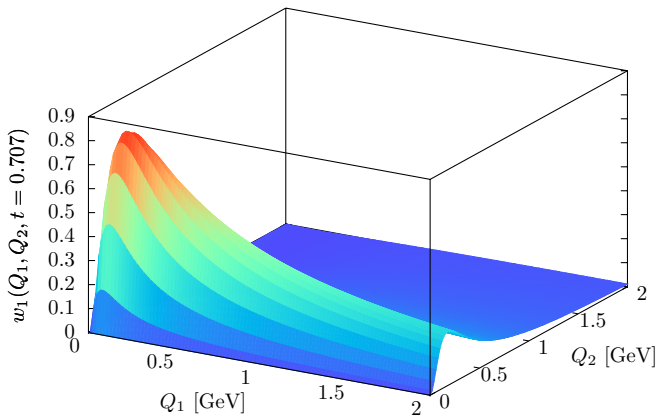

$t = 0.707, \quad \theta = 45°$

Low momentum region most important. Peak around $Q_1 \sim 0.2$ GeV, $Q_2 \sim 0.15$ GeV.

Despite the appearance in the plots, the slopes along the two axis and along the diagonal (at $Q_1 = Q_2 = 0$) vanish.

For $t > -0.85$ ($\theta < 150°$) a ridge develops along Q_1 direction for $Q_2 \sim 0.2$ GeV.

Leads for constant form factor to a divergence $\ln^2 \Lambda$ for some momentum cutoff Λ.

Realistic form factor falls off for large Q_i and integral $a_\mu^{\mathrm{HLbL};\pi^0(1)}$ will be convergent.

Weight function $w_2(Q_1, Q_2, t)$

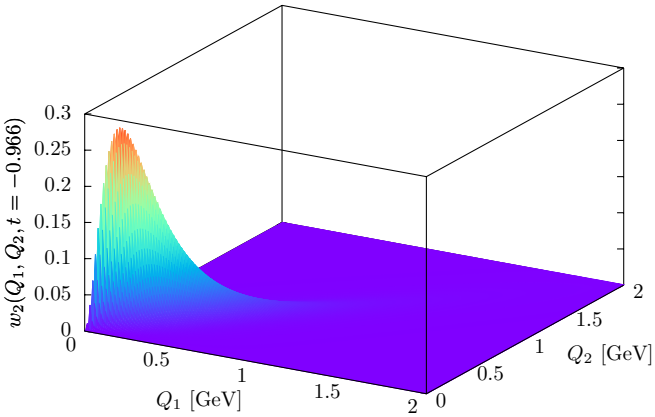

$t = -0.966, \quad \theta = 165°$

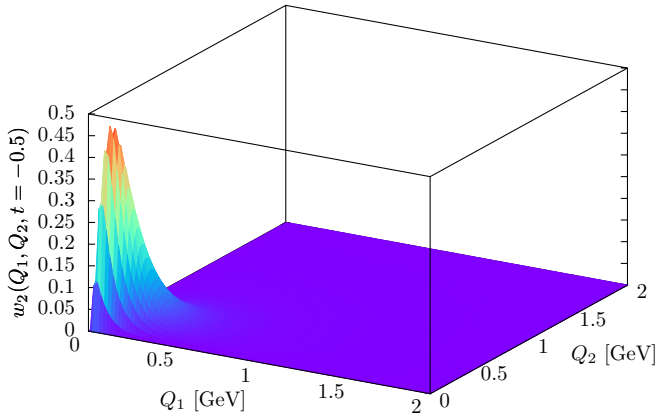

$t = -0.5, \quad \theta = 120°$

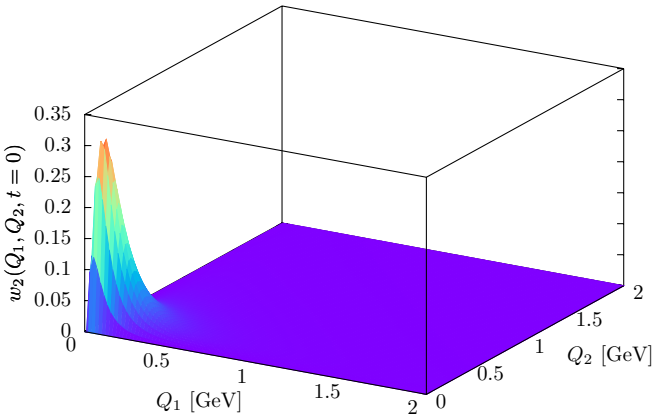

$t = 0, \quad \theta = 90°$

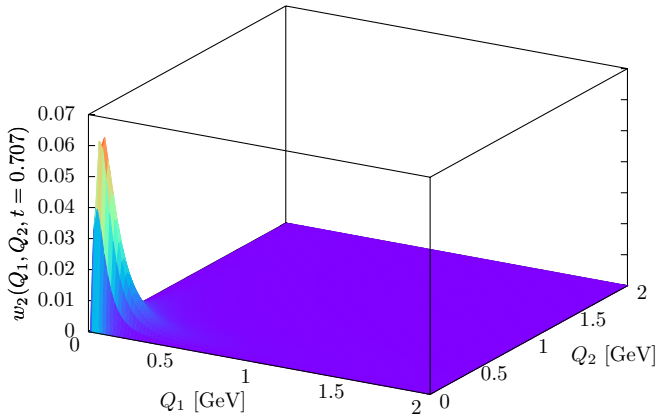

$t = 0.707, \quad \theta = 45°$

w_2 is about a factor 10 smaller than w_1 and there is no ridge in one direction. Note that $w_2(Q_1, Q_2, t)$ is symmetric under $Q_1 \leftrightarrow Q_2$. Peak for $Q_1 = Q_2 \sim 0.15$ GeV for t near -1, peak moves to lower values $Q_1 = Q_2 = 0.04$ GeV for t near 1.
Again the slopes along the two axis and along the diagonal (at $Q_1 = Q_2 = 0$) vanish.

Even for constant form factor, one obtains finite result: $\left(\frac{\alpha}{\pi}\right)^3 a_{\mu;\mathrm{WZW}}^{\mathrm{HLbL};\pi^0(2)} \sim 2.5 \times 10^{-11}$

Variation of $w_{1,2}(Q_1, Q_2, t)$ with $t = \cos\theta$ for selected Q_1, Q_2

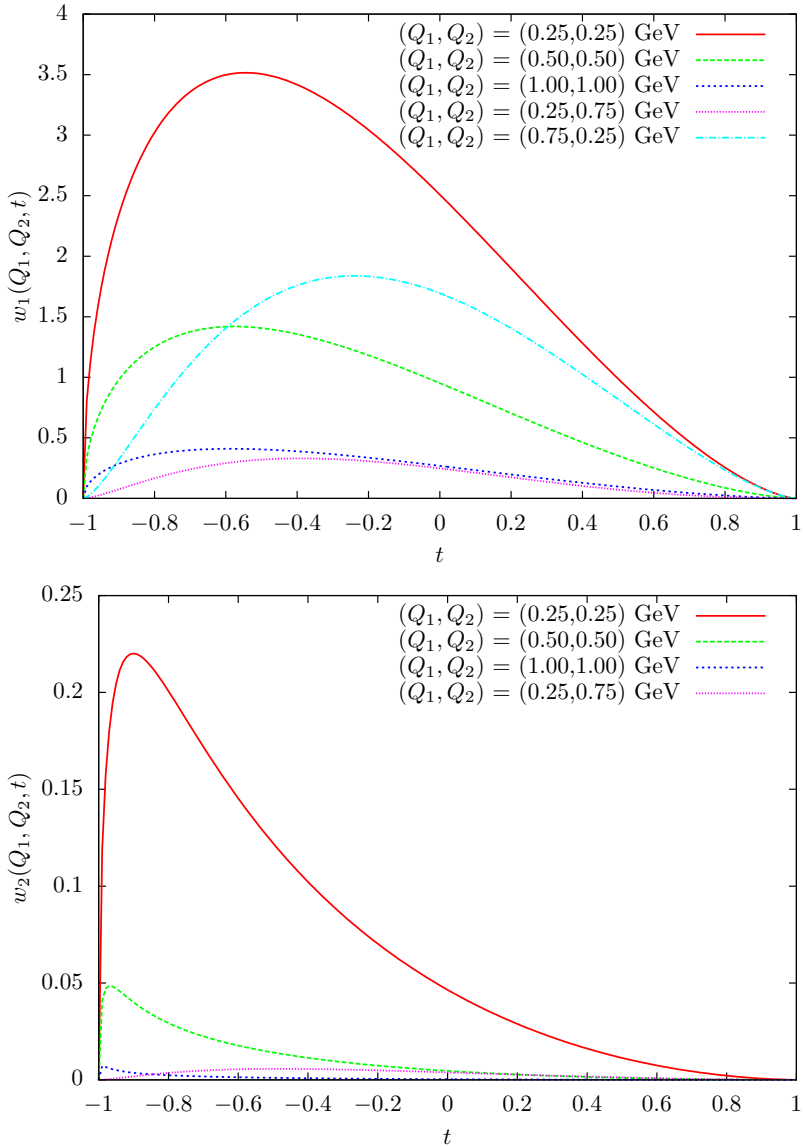

Strong enhancement for $Q_1 = Q_2$ for negative t, when the original four-vectors $(Q_1)_\mu$ and $(Q_2)_\mu$ become more antiparallel. For $Q_1 = Q_2$ both weight functions have infinite slope at $t = -1$. Overall, weight functions get smaller for larger $Q_i > 0.5$ GeV.

For illustration: LMD+V and VMD models

- Since the integral $a_\mu^{\mathrm{HLbL};\pi^0(1)}$ is divergent without form factors, we take two simple models for illustration to see where are the relevant momentum regions in the integral.
- Of course, in the end, the models have to be replaced by experimental data on the doubly-virtual form factor $\mathcal{F}_{\pi^0\gamma^*\gamma^*}(-Q_1^2,-Q_2^2)$.
- LMD+V model (Lowest Meson Dominance + V) is a generalization of Vector Meson Dominance (VMD) in the framework of large-N_C QCD, which respects (some) short-distance constraints from the operator product expansion (OPE).
- Main difference is doubly-virtual case: VMD model violates OPE, falls off too fast:

$$\mathcal{F}^{\mathrm{VMD}}_{\pi^0\gamma^*\gamma^*}(-Q^2,-Q^2) \sim \frac{1}{Q^4} \qquad \text{for large } Q^2$$

$$\mathcal{F}^{\mathrm{LMD+V}}_{\pi^0\gamma^*\gamma^*}(-Q^2,-Q^2) \sim \mathcal{F}^{\mathrm{OPE}}_{\pi^0\gamma^*\gamma^*}(-Q^2,-Q^2) \sim \frac{1}{Q^2} \qquad \text{for large } Q^2$$

Contributions to $a_\mu^{\mathrm{HLbL};\pi^0}$ from different momentum regions

$$a_{\mu;\mathrm{LMD+V}}^{\mathrm{HLbL};\pi^0} = 62.9 \times 10^{-11}$$

$$a_{\mu;\mathrm{VMD}}^{\mathrm{HLbL};\pi^0} = 57.0 \times 10^{-11}$$

Integrate over individual momentum bins:

$$\int_{Q_{1,\min}}^{Q_{1,\max}} dQ_1 \int_{Q_{2,\min}}^{Q_{2,\max}} dQ_2 \int_{-1}^{1} dt$$

Contribution of individual bins to total:

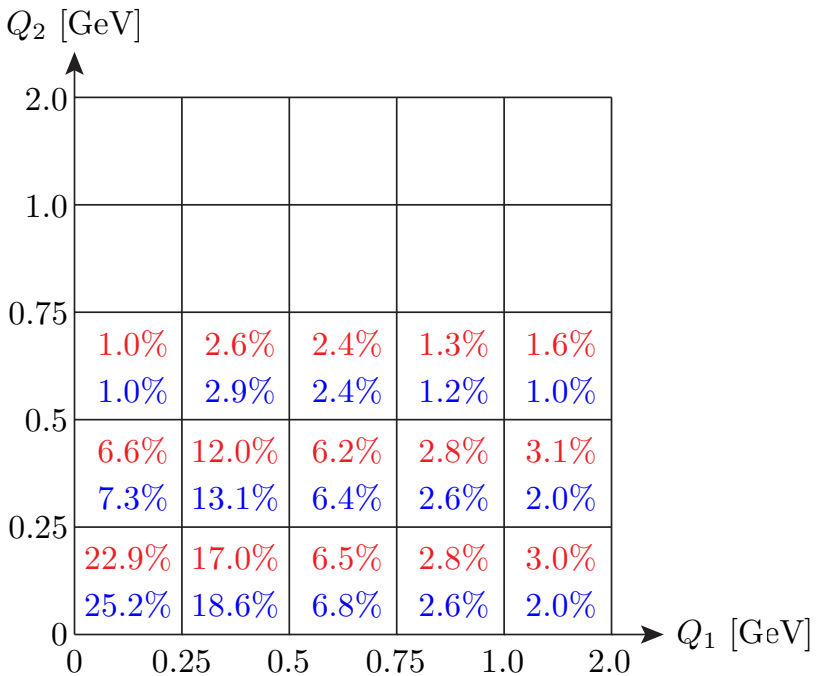

Bin sizes vary. No entry: contribution $< 1\%$. Asymmetry in (Q_1, Q_2)-plane with larger contributions below diagonal reflects ridge-like structure in dominant $w_1(Q_1, Q_2, t)$.

Pion-pole contribution $a_\mu^{\mathrm{HLbL};\pi^0} \times 10^{11}$ for LMD+V and VMD form factors obtained with momentum cutoff Λ (integration over square). In brackets, relative contribution of the total obtained with $\Lambda = 20$ GeV.

Λ [GeV]	LMD+V	VMD
0.25	14.4 (22.9%)	14.4 (25.2%)
0.5	36.8 (58.5%)	36.6 (64.2%)
0.75	48.5 (77.1%)	47.7 (83.8%)
1.0	54.1 (86.0%)	52.6 (92.3%)
1.5	58.8 (93.4%)	55.8 (97.8%)
2.0	60.5 (96.2%)	56.5 (99.2%)
5.0	62.5 (99.4%)	56.9 (99.9%)
20.0	62.9 (100%)	57.0 (100%)

Region below $\Lambda = 0.5$ GeV gives more than half of the contribution: 59% for LMD+V, 64% for VMD.

Bulk of result below $\Lambda = 1$ GeV: 86% for LMD+V, 92% for VMD.

VMD: faster fall-off, contributions more concentrated at lower momenta compared to LMD+V.

Impact of form factor uncertainties

Rough description of measurement errors for single-virtual form factor

$$\mathcal{F}_{\pi^0\gamma^*\gamma^*}(-Q^2,0)$$
$$\to \mathcal{F}_{\pi^0\gamma^*\gamma^*}(-Q^2,0)\,(1+\delta_1(Q))$$

where we assumed the following momentum dependent errors for $\delta_1(Q)$:

Momentum range [GeV]	$\delta_1(Q)$
$0 \le Q < 0.5$	5% [2%]
$0.5 \le Q < 1$	7.5% [4%]
$1 \le Q < 2$	10%
$2 \le Q$	12.5%

Based on measurements by CELLO, CLEO and ongoing analysis by BES III. For lowest bin, assumed error. [ ]: $\Gamma(\pi^0 \to \gamma\gamma)$ and DR for TFF at low energies (Hoferichter et al. '14).

Description of measurement errors for the double-virtual form factor

$$\mathcal{F}_{\pi^0\gamma^*\gamma^*}(-Q_1^2,-Q_2^2)$$
$$\to \mathcal{F}_{\pi^0\gamma^*\gamma^*}(-Q_1^2,-Q_2^2)\,(1+\delta_2(Q_1,Q_2))$$

Monte Carlo simulations by Mainz group for $e^+e^- \to e^+e^-\gamma^*\gamma^* \to e^+e^-\pi^0$ at BES III with LMD+V in EKHARA (Czyż, Ivashyn '11).

Based on these Monte Carlo simulations (for signal process only !), the momentum dependent errors $\delta_2(Q_1, Q_2)$ are assumed as follows:

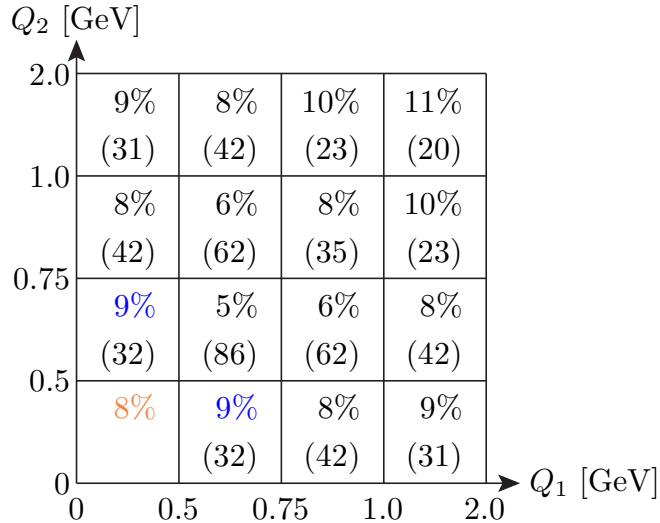

Note the unequal bin sizes ! In brackets: number of MC events N_i in each bin $\sim$ $\sigma \sim \mathcal{F}^2_{\pi^0\gamma^*\gamma^*} \Rightarrow \delta\mathcal{F}_{\pi^0\gamma^*\gamma^*} = \sqrt{N_i}/(2N_i)$ (total: 600 events). For lowest bin, assumed error ("extrapolation" from boundary values (average of neighboring bins)), no events in simulation (detector acceptance).

Number of events and corresponding precision for $\mathcal{F}_{\pi^0\gamma^*\gamma^*}(-Q_1^2,-Q_2^2)$ should be achievable with current data set at BES III plus a few more years of data taking.

Impact of form factor uncertainties (continued)

LMD+V model [VMD model] (relative errors very similar)

$a_{\mu;\mathrm{LMD+V}}^{\mathrm{HLbL};\pi^0} = 62.9 \times 10^{-11}$ $\left[a_{\mu;\mathrm{VMD}}^{\mathrm{HLbL};\pi^0} = 57.0 \times 10^{-11}\right]$

$\delta a_\mu^{\mathrm{HLbL};\pi^0} \times 10^{11}$	Relative error	Comment
$^{+9.0}_{-8.3}$ $\left[^{+7.9}_{-7.3}\right]$	$^{+14.2\%}_{-13.2\%}$ $\left[^{+13.9\%}_{-12.8\%}\right]$	Given δ_1, δ_2
$^{+2.7}_{-2.7}$ $\left[^{+2.5}_{-2.4}\right]$	$^{+4.3\%}_{-4.2\%}$ $\left[^{+4.4\%}_{-4.3\%}\right]$	Bin $Q < 0.5$ GeV in $\delta_1 = 5\%$, rest: $\delta_{1,2} = 0$
$^{+0.8}_{-0.7}$ $\left[^{+0.6}_{-0.5}\right]$	$^{+1.2\%}_{-1.1\%}$ $\left[^{+1.1\%}_{-1.0\%}\right]$	Bins $Q \geq 0.5$ GeV in δ_1 as given, rest: $\delta_{1,2} = 0$
$^{+2.8}_{-2.8}$ $\left[^{+2.8}_{-2.7}\right]$	$^{+4.5\%}_{-4.4\%}$ $\left[^{+4.9\%}_{-4.8\%}\right]$	Bin $Q_{1,2} < 0.5$ GeV in $\delta_2 = 8\%$, rest: $\delta_{1,2} = 0$
$^{+2.5}_{-2.4}$ $\left[^{+1.8}_{-1.8}\right]$	$^{+3.9\%}_{-3.8\%}$ $\left[^{+3.2\%}_{-3.1\%}\right]$	Bins $Q_{1,2} \geq 0.5$ GeV in δ_2 as given, rest: $\delta_{1,2} = 0$
$^{+6.9}_{-6.6}$ $\left[^{+6.0}_{-5.8}\right]$	$^{+11.0\%}_{-10.5\%}$ $\left[^{+10.6\%}_{-10.1\%}\right]$	Given δ_1, δ_2, but two lowest bins in δ_1: $2\%, 4\%$
$^{+7.9}_{-7.3}$ $\left[^{+6.8}_{-6.3}\right]$	$^{+12.5\%}_{-11.7\%}$ $\left[^{+11.9\%}_{-11.1\%}\right]$	Given δ_1, δ_2, but lowest bin in δ_2: $8\% \to 5\%$
$^{+7.6}_{-7.1}$ $\left[^{+6.5}_{-6.1}\right]$	$^{+12.1\%}_{-11.3\%}$ $\left[^{+11.5\%}_{-10.7\%}\right]$	In addition: bins in δ_2 close to lowest bin $9\% \to 5\%$

For LMD+V FF [VMD FF], region $Q_{1,2} < 0.5$ GeV gives 59% [64%] to total.

In order to reach goal of 10% error for $a_\mu^{\mathrm{HLbL};\pi^0}$, it would help, if one could measure double-virtual TFF in region $Q_{1,2} < 0.5$ GeV, constrain it using DR or with informations from Lattice QCD (assumed error of 8% in lowest bin !).

Recall model calculations: $a_\mu^{\mathrm{HLbL};\pi^0} = (50 - 80) \times 10^{-11} = (65 \pm 15) \times 10^{-11}$ $(\pm 23\%)$.

Pole contributions from η and η'

Only dependence on pseudoscalars appears in weight functions through pseudoscalar mass m_P in propagators:

In weight function $w_1(Q_1, Q_1, t)$: $\dfrac{1}{Q_2^2 + m_P^2}$

In weight function $w_2(Q_1, Q_1, t)$: $\dfrac{1}{(Q_1 + Q_2)^2 + m_P^2} = \dfrac{1}{Q_1^2 + 2Q_1 Q_2 t + Q_2^2 + m_P^2}$

Two effects:

1. Shifts the relevant momentum regions (peaks, ridges) to higher momenta for η compared to π^0 and even higher for η'.

2. Leads to suppression in absolute size of the weight functions due to larger masses in the propagators. For the bulk of the weight functions we have the approximate relations:

$$w_1|_\eta \approx \frac{1}{6}\, w_1|_{\pi^0}$$

$$w_1|_{\eta'} \approx \frac{1}{2.5}\, w_1|_\eta$$

Weight functions for η

Weight function $w_1(Q_1, Q_2, t)$

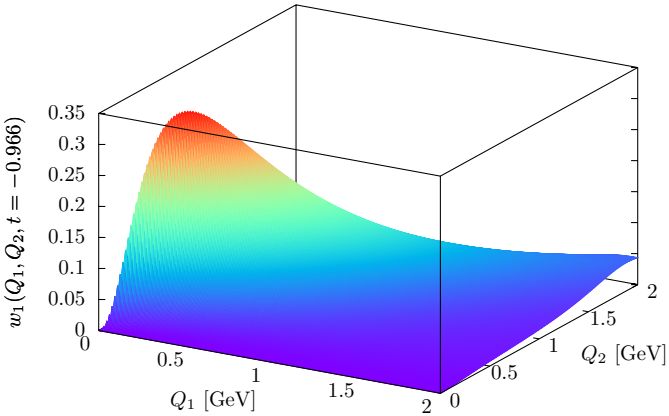

$t = -0.966, \quad \theta = 165°$

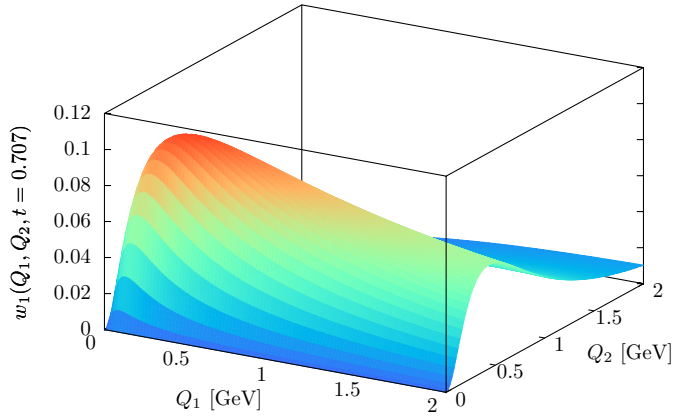

$t = 0.707, \quad \theta = 45°$

Weight function $w_2(Q_1, Q_2, t)$

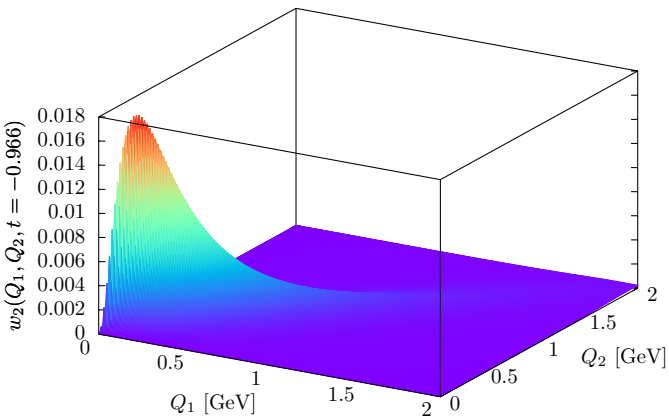

$t = -0.966, \quad \theta = 165°$

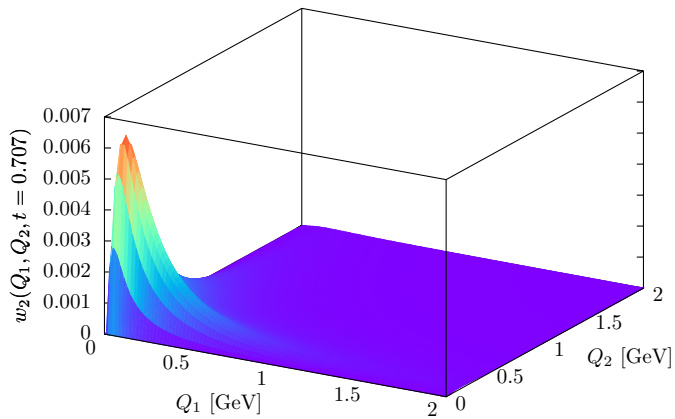

$t = 0.707, \quad \theta = 45°$

Peaks and ridges have broadened compared to π^0.

Peak for w_1 around $Q_1 \sim 0.32 - 0.37$ GeV, $Q_2 \sim 0.22 - 0.33$ GeV. w_2 about a factor 20 smaller than w_1. Peak for w_2 around $Q_1 = Q_2 \sim 0.14$ GeV for t near -1, moves down to $Q_1 = Q_2 = 0.06$ GeV for t near 1.

w_2: finite result for constant form factor $\left(\frac{\alpha}{\pi}\right)^3 a_{\mu;\mathrm{WZW}}^{\mathrm{HLbL};\eta(2)} = 0.78 \times 10^{-11}$

Weight functions for η'

Weight function $w_1(Q_1, Q_2, t)$

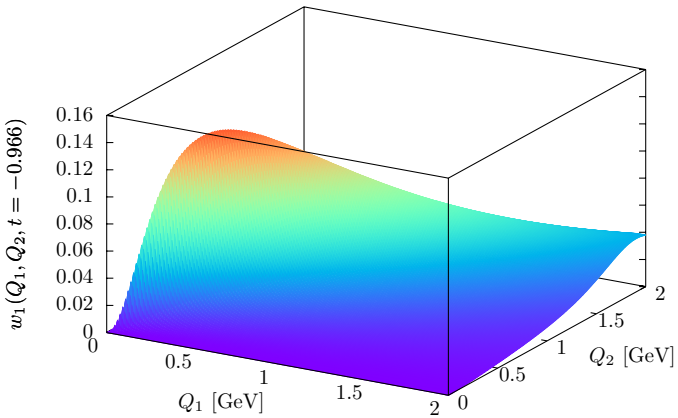

$t = -0.966, \quad \theta = 165°$

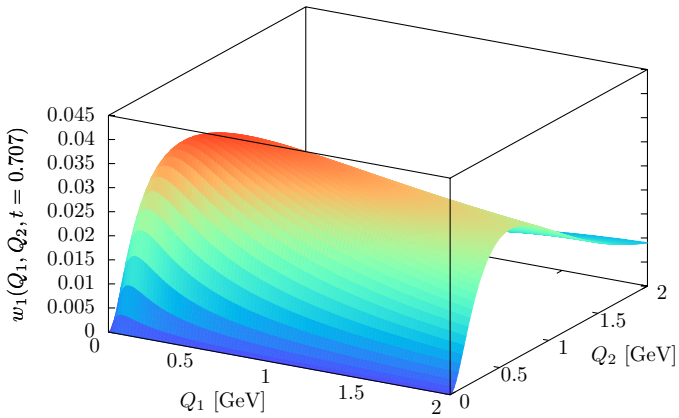

$t = 0.707, \quad \theta = 45°$

Weight function $w_2(Q_1, Q_2, t)$

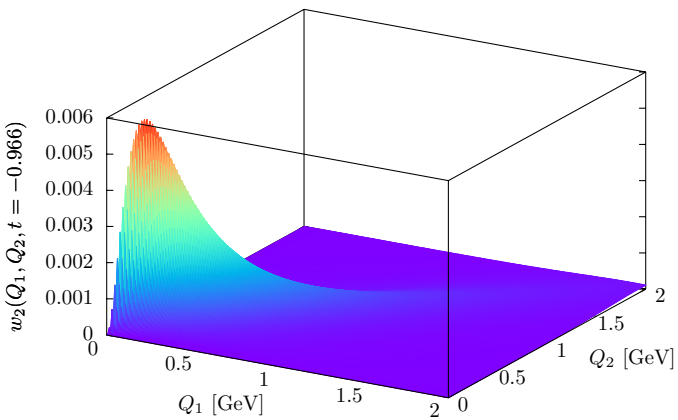

$t = -0.966, \quad \theta = 165°$

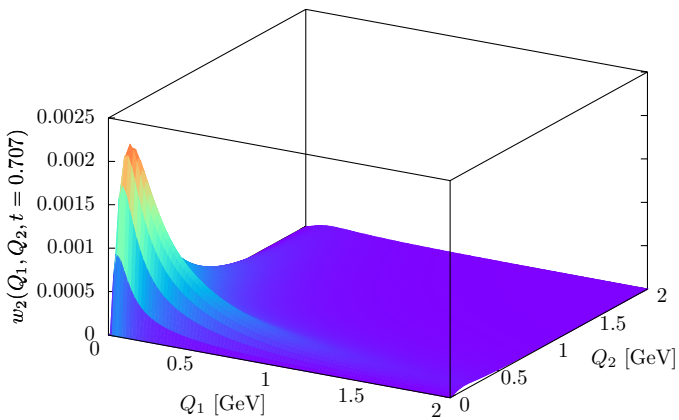

$t = 0.707, \quad \theta = 45°$

Peaks and ridges have broadened even more.

Peak for w_1 around $Q_1 \sim 0.41 - 0.51$ GeV, $Q_2 \sim 0.31 - 0.43$ GeV. w_2 about a factor 20 smaller than w_1. Peak for w_2 around $Q_1 = Q_2 \sim 0.14$ GeV for t near -1, moves down to $Q_1 = Q_2 = 0.07$ GeV for t near 1.

w_2: finite result for constant form factor $\left(\frac{\alpha}{\pi}\right)^3 a_{\mu;\mathrm{WZW}}^{\mathrm{HLbL};\eta'(2)} = 0.65 \times 10^{-11}$

Contributions to $a_\mu^{\mathrm{HLbL};\eta}$ and $a_\mu^{\mathrm{HLbL};\eta'}$ from different momentum regions

Use VMD model with adapted parameter F_{P} to describe $\Gamma(\mathrm{P}\to\gamma\gamma)$ and M_V from fit of $\mathcal{F}_{\mathrm{P}\gamma^*\gamma^*}(-Q^2,0)$ to CLEO data:

$$F_\eta = 93.0\ \text{MeV}, \quad M_V = 775\ \text{MeV}$$
$$F_{\eta'} = 74.0\ \text{MeV}, \quad M_V = 859\ \text{MeV}$$

One obtains (Knecht, AN '02):

$$a_{\mu;\mathrm{VMD}}^{\mathrm{HLbL};\eta} = 14.5\times10^{-11}$$
$$a_{\mu;\mathrm{VMD}}^{\mathrm{HLbL};\eta'} = 12.5\times10^{-11}$$

Contribution of individual bins to total (bin sizes vary; no entry: contribution $< 1\%$):

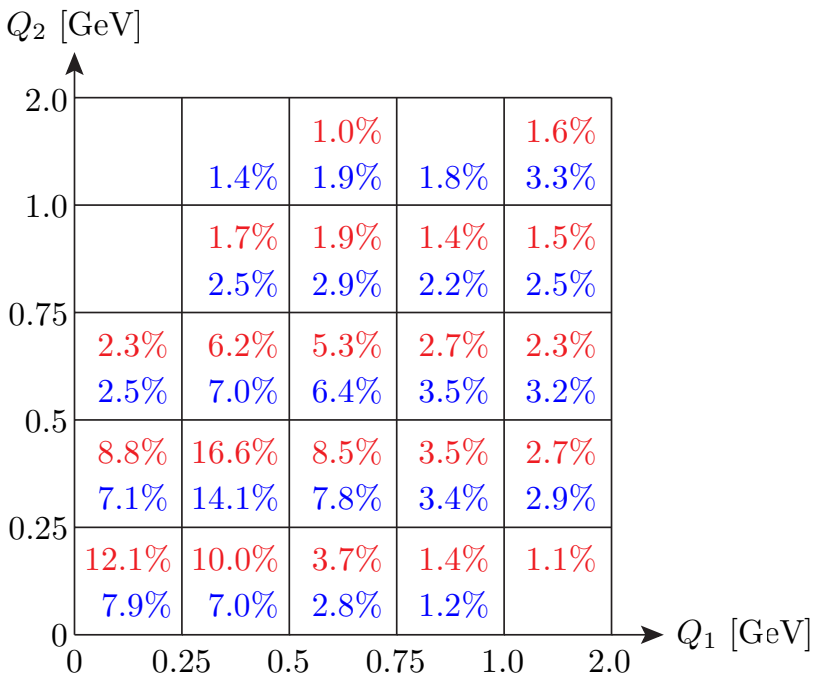

Pole contributions $a_\mu^{\mathrm{HLbL};\eta}\times10^{11}$ and $a_\mu^{\mathrm{HLbL};\eta'}\times10^{11}$ with the VMD form factor obtained with a momentum cutoff Λ. In brackets, relative contribution of the total obtained with $\Lambda = 20$ GeV.

Λ [GeV]	η	η'
0.25	1.8 (12.1%)	1.0 (7.9%)
0.5	6.9 (47.5%)	4.5 (36.1%)
0.75	10.7 (73.4%)	7.8 (62.5%)
1.0	12.6 (86.6%)	9.9 (79.1%)
1.5	14.0 (96.1%)	11.7 (93.1%)
2.0	14.3 (98.6%)	12.2 (97.4%)
5.0	14.5 (100%)	12.5 (99.9%)
20.0	14.5 (100%)	12.5 (100%)

Region below $\Lambda = 0.25$ GeV gives very small contribution to total: 12% for η, 8% for η'.

Region below $\Lambda = 0.5$ GeV gives: 48% for η, 36% for η'.

Bulk of result below $\Lambda = 1.5$ GeV: 96% for η, 93% for η'.

Impact of form factor uncertainties

The momentum dependent errors $\delta_2(Q_1, Q_2)$ are assumed as follows:

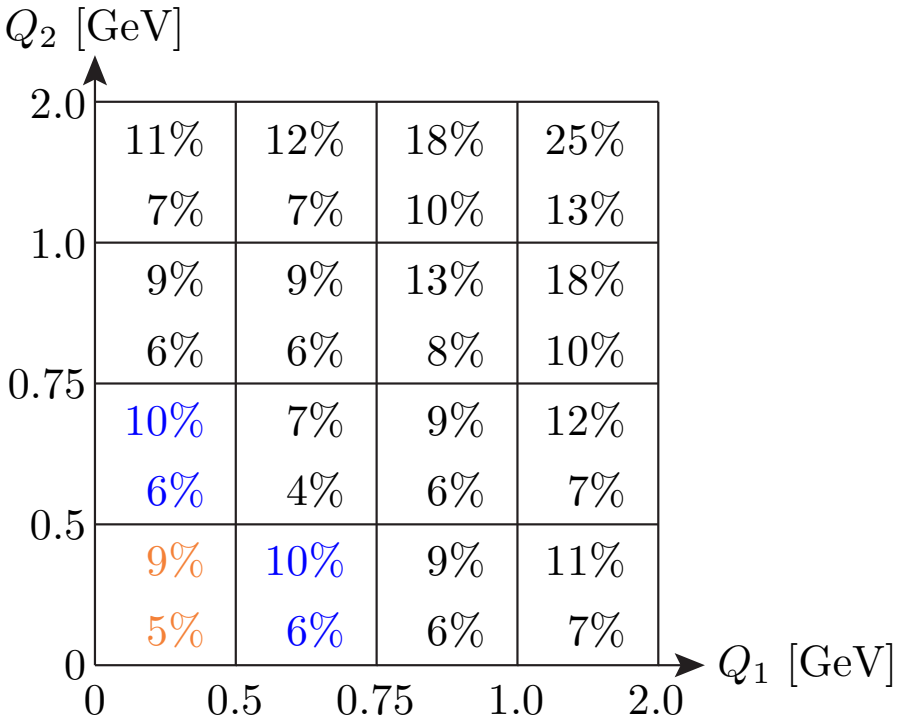

Top line in bin: η-meson (total: 345 events).
Bottom line: η'-meson (total: 902 events).
For lowest bin, assumed error ("extrapolation" from boundary values (average of neighboring bins)), no events in simulation (detector acceptance).
Note again the unequal bin sizes.

Monte Carlo simulations for BES III (Mainz group) based on VMD model in EKHARA (Czyż, Ivashyn '11)

Number of events and corresponding precision for $\mathcal{F}_{\mathrm{P}\gamma^*\gamma^*}(-Q_1^2, -Q_2^2)$ should be achievable with current data set plus a few more years of data taking, although the separation of signal and background will be more difficult for η and η' than for the pion.

For simplicity, for the single-virtual form factor we assume the same errors $\delta_1(Q)$ as for the pion (but no precise dispersive evaluation available yet).

Impact of form factor uncertainties (continued)

VMD model (for illustration)

$a_{\mu;\mathrm{VMD}}^{\mathrm{HLbL};\eta} = 14.5 \times 10^{-11}$ $\left[a_{\mu;\mathrm{VMD}}^{\mathrm{HLbL};\eta'} = 12.5 \times 10^{-11}\right]$

$\delta a_\mu^{\mathrm{HLbL};\eta[\eta']} \times 10^{11}$	Relative error	Comment
$^{+2.6}_{-2.3}$ $[^{+1.7}_{-1.6}]$	$^{+17.5\%}_{-16.1\%}$ $[^{+13.6\%}_{-12.6\%}]$	Given δ_1, δ_2
$^{+0.5}_{-0.5}$ $[^{+0.4}_{-0.3}]$	$^{+3.5\%}_{-3.4\%}$ $[^{+2.8\%}_{-2.7\%}]$	Bin $Q < 0.5$ GeV in $\delta_1 = 5\%$, rest: $\delta_{1,2} = 0$
$^{+0.4}_{-0.4}$ $[^{+0.5}_{-0.5}]$	$^{+2.5\%}_{-2.4\%}$ $[^{+3.7\%}_{-3.6\%}]$	Bins $Q \geq 0.5$ GeV in δ_1 as given, rest: $\delta_{1,2} = 0$
$^{+0.6}_{-0.6}$ $[^{+0.2}_{-0.2}]$	$^{+4.0\%}_{-4.0\%}$ $[^{+1.7\%}_{-1.7\%}]$	Bin $Q_{1,2} < 0.5$ GeV: $\delta_2 = 9\%[5\%]$, rest: $\delta_{1,2} = 0$
$^{+1.0}_{-1.0}$ $[^{+0.6}_{-0.6}]$	$^{+7.0\%}_{-6.8\%}$ $[^{+5.1\%}_{-5.0\%}]$	Bins $Q_{1,2} \geq 0.5$ GeV in δ_2 as given, rest: $\delta_{1,2} = 0$
$^{+2.4}_{-2.2}$ $[^{+1.7}_{-1.5}]$	$^{+16.6\%}_{-15.2\%}$ $[^{+13.3\%}_{-12.3\%}]$	Given δ_1, δ_2, lowest bin in δ_2: $9\%[5\%] \to 7\%[4\%]$
$^{+2.3}_{-2.2}$ $[^{+1.6}_{-1.5}]$	$^{+16.1\%}_{-14.8\%}$ $[^{+12.9\%}_{-12.1\%}]$	In addition: bins in δ_2 with $10\%[6\%] \to 7\%[4\%]$

For η $[\eta']$, region $Q_{1,2} < 0.5$ GeV gives 48% [36%] to total.

$a_\mu^{\mathrm{HLbL};\eta}$: in order to reach goal of 10% error, it would help, if one could measure double-virtual TFF in region $Q_{1,2} < 0.5$ GeV.

$a_\mu^{\mathrm{HLbL};\eta'}$: information for $0.5 \leq Q_{1,2} \leq 1$GeV would be helpful.

Dispersive approach ? Lattice QCD ?

Conclusions and Outlook

- Started from 3-dimensional integral representation for pseudoscalar-pole contribution $a_\mu^{\mathrm{HLbL;P}}, \mathrm{P} = \pi^0, \eta, \eta'$, derived in Jegerlehner, AN '09.
- Separates the generic kinematics with model-independent weight functions $w_{1,2}(Q_1, Q_2, t)$ from doubly-virtual form factors $\mathcal{F}_{\mathrm{P}\gamma^*\gamma^*}(-Q_1^2, -Q_2^2)$, which can, in principle, be obtained from measurements.
- Relevant momentum regions from weight functions: below about 1 GeV for π^0, below about 1.5 GeV for η and η'.
- Showed impact of measurement errors of the doubly-virtual form factor on final result for $a_\mu^{\mathrm{HLbL;P}}$ based on Monte-Carlo simulations for the signal in the process $e^+e^- \to e^+e^-\gamma^*\gamma^* \to e^+e^-\mathrm{P}$ at BES III. For illustration used two simple form factor models (LMD+V, VMD) for π^0, VMD for η, η'.
- With precision reachable for $\mathcal{F}_{\mathrm{P}\gamma^*\gamma^*}(-Q_1^2, -Q_2^2)$ from BES III in a few more years and with other (assumed) input in particular at $Q_{1,2} \leq 0.5$ GeV:

$$\begin{aligned} \delta a_\mu^{\mathrm{HLbL};\pi^0} &= 14\% \ \ [11\%] \\ \delta a_\mu^{\mathrm{HLbL};\eta} &= 18\% \\ \delta a_\mu^{\mathrm{HLbL};\eta'} &= 14\% \end{aligned}$$

  [ ]: with dispersion relation (DR) for single-virtual $\mathcal{F}_{\pi^0\gamma^*\gamma^*}(-Q^2, 0)$
- In order for dispersive approach to HLbL to be successful, one needs π^0, η^0, η'-pole contributions to 10% precision $\Rightarrow$ needs to improve uncertainties !
- Future: more work needed to estimate effect of backgrounds and analysis cuts at BES III. Further informations needed for form factors $\mathcal{F}_{\mathrm{P}\gamma^*\gamma^*}(-Q_1^2, -Q_2^2)$, in particular for low $Q_{1,2} \leq 1$ GeV from other experiments (KLOE 2 ? Belle 2 ?), from DR for form factors and maybe from Lattice QCD.

Backup slides

HLbL scattering: Summary of selected results

Some results for the various contributions to $a_\mu^{\rm HLbL} \times 10^{11}$:

Contribution	BPP	HKS, HK	KN	MV	BP, MdRR	PdRV	N, JN
π^0, η, η'	85±13	82.7±6.4	83±12	114±10	–	114±13	99 ± 16
axial vectors	2.5±1.0	1.7±1.7	–	22±5	–	15±10	22±5
scalars	−6.8±2.0	–	–	–	–	−7±7	−7±2
π, K loops	−19±13	−4.5±8.1	–	–	–	−19±19	−19±13
π, K loops +subl. N_C	–	–	–	0±10	–	–	–
quark loops	21±3	9.7±11.1	–	–	–	2.3 (c-quark)	21±3
Total	83±32	89.6±15.4	80±40	136±25	110±40	105 ± 26	116 ± 39

BPP = Bijnens, Pallante, Prades '95, '96, '02; HKS = Hayakawa, Kinoshita, Sanda '95, '96; HK = Hayakawa, Kinoshita '98, '02; KN = Knecht, AN '02; MV = Melnikov, Vainshtein '04; BP = Bijnens, Prades '07; MdRR = Miller, de Rafael, Roberts '07; PdRV = Prades, de Rafael, Vainshtein '09; N = AN '09, JN = Jegerlehner, AN '09

- Pseudoscalar-exchanges dominate numerically. Other contributions not negligible. Cancellation between π, K-loops and quark loops !
- PdRV: Analyzed results obtained by different groups with various models and suggested new estimates for some contributions (shifted central values, enlarged errors). Do not consider dressed light quark loops as separate contribution ! Assume it is already taken into account by using short-distance constraint of MV '04 on pseudoscalar-pole contribution. Added all errors in quadrature !
- N, JN: New evaluation of pseudoscalar exchange contribution imposing new short-distance constraint on off-shell form factors. Took over most values from BPP, except axial vectors from MV. Added all errors linearly.

Data-driven approach to HLbL using dispersion relations (DR)

- Strategy: Split contributions to HLbL into two parts:

  I: Data-driven evaluation using DR (hopefully numerically dominant):

  (1) π^0, η, η' poles

  (2) $\pi\pi$ intermediate state

  II: Model dependent evaluation (hopefully numerically subdominant):

  (1) Axial vectors (3π-intermediate state), ...

  (2) Quark-loop, matching with pQCD

  Error goals: Part I: 10% precision (data driven), Part II: 30% precision.
  To achieve overall error of about 20% ($\delta a_\mu^{\mathrm{HLbL}} = 20 \times 10^{-11}$).
  More efforts needed to get down to 10% overall precision !

- Colangelo et al.:
  Classify intermediate states in four-point function. Then project onto $g-2$.

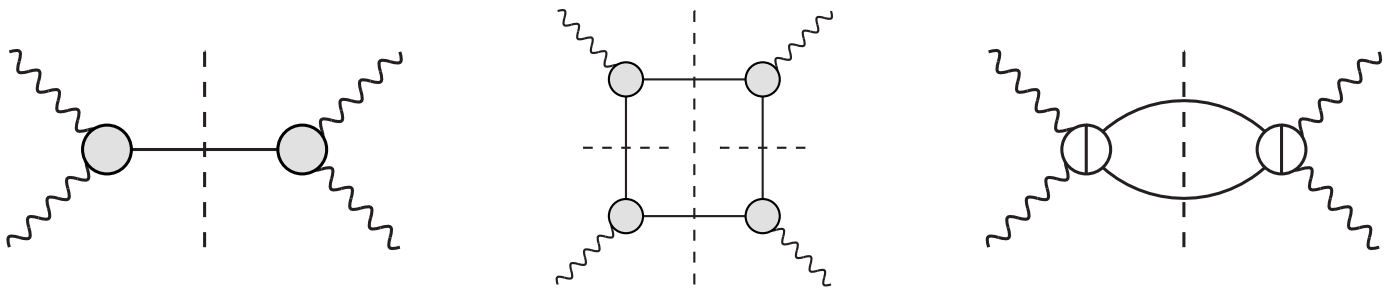

- Pauk, Vanderhaeghen:
  Write DR directly for Pauli form factor $F_2(k^2)$.

Expressions for weight functions $w_{1,2}(Q_1, Q_2, t)$

Jegerlehner, AN '09

$$w_1(Q_1, Q_2, t) = \left(-\frac{2\pi}{3}\right)\sqrt{1-t^2}\,\frac{Q_1^3 Q_2^3}{Q_2^2+m_\pi^2}\,I_1(Q_1, Q_2, t)$$

$$w_2(Q_1, Q_2, t) = \left(-\frac{2\pi}{3}\right)\sqrt{1-t^2}\,\frac{Q_1^3 Q_2^3}{Q_3^2+m_\pi^2}\,I_2(Q_1, Q_2, t)$$

$$\begin{aligned}
I_1(Q_1, Q_2, t) = X(Q_1, Q_2, t)\Big(&8\,P_1\,P_2\,(Q_1\cdot Q_2) - 2\,P_1\,P_3\,(Q_2^4/m_\mu^2 - 2\,Q_2^2) - 2\,P_1\,(2 - Q_2^2/m_\mu^2 + 2\,(Q_1\cdot Q_2)/m_\mu^2)\\
&+4\,P_2\,P_3\,Q_1^2 - 4\,P_2 - 2\,P_3\,(4 + Q_1^2/m_\mu^2 - 2\,Q_2^2/m_\mu^2) + 2/m_\mu^2\Big)\\
&-2\,P_1\,P_2\,(1 + (1-R_{m1})\,(Q_1\cdot Q_2)/m_\mu^2) + P_1\,P_3\,(2 - (1-R_{m1})\,Q_2^2/m_\mu^2) + P_1\,(1-R_{m1})/m_\mu^2\\
&+P_2\,P_3\,(2 + (1-R_{m1})^2\,(Q_1\cdot Q_2)/m_\mu^2) + 3\,P_3\,(1-R_{m1})/m_\mu^2
\end{aligned}$$

$$\begin{aligned}
I_2(Q_1, Q_2, t) = X(Q_1, Q_2, t)\Big(&4\,P_1\,P_2\,(Q_1\cdot Q_2) + 2\,P_1\,P_3\,Q_2^2 - 2\,P_1 + 2\,P_2\,P_3\,Q_1^2 - 2\,P_2 - 4P_3 - 4/m_\mu^2\Big)\\
&-2\,P_1\,P_2 - 3\,P_1\,(1-R_{m2})/(2m_\mu^2) - 3\,P_2\,(1-R_{m1})/(2m_\mu^2) - P_3\,(2 - R_{m1} - R_{m2})/(2m_\mu^2)\\
&+P_1\,P_3\,(2 + 3\,(1-R_{m2})\,Q_2^2/(2m_\mu^2) + (1-R_{m2})^2\,(Q_1\cdot Q_2)/(2m_\mu^2))\\
&+P_2\,P_3\,(2 + 3\,(1-R_{m1})\,Q_1^2/(2m_\mu^2) + (1-R_{m1})^2\,(Q_1\cdot Q_2)/(2m_\mu^2))
\end{aligned}$$

where $Q_3^2 = (Q_1+Q_2)^2$, $\quad Q_1\cdot Q_2 = Q_1 Q_2\cos\theta$, $\quad t = \cos\theta$

$P_1^2 = 1/Q_1^2$, $\quad P_2^2 = 1/Q_2^2$, $\quad P_3^2 = 1/Q_3^2$, $\quad X(Q_1, Q_2, t) = \frac{1}{Q_1 Q_2\, x}\arctan\left(\frac{zx}{1-zt}\right)$,

$x = \sqrt{1-t^2}$, $\quad z = \frac{Q_1 Q_2}{4m_\mu^2}\,(1-R_{m1})\,(1-R_{m2})$, $\quad R_{mi} = \sqrt{1+4m_\mu^2/Q_i^2}$

Locations and values of maxima of $w_{1,2}(Q_1, Q_2, t)$

θ ($t = \cos\theta$)	Max. w_1	Q_1 [GeV]	Q_2 [GeV]	Max. w_2	$Q_1 = Q_2$ [GeV]
175° (-0.996)	0.592	0.163	0.163	0.100	0.142
165° (-0.966)	1.734	0.164	0.162	0.277	0.132
150° (-0.866)	3.197	0.166	0.158	0.441	0.114
135° (-0.707)	4.176	0.171	0.153	0.494	0.099
120° (-0.5)	4.559	0.176	0.146	0.471	0.087
105° (-0.259)	4.349	0.182	0.139	0.403	0.078
90° (0.0)	3.664	0.187	0.130	0.312	0.070
75° (0.259)	2.702	0.189	0.122	0.218	0.063
60° (0.5)	1.691	0.187	0.114	0.132	0.057
45° (0.707)	0.840	0.180	0.106	0.064	0.050
30° (0.866)	0.283	0.168	0.099	0.021	0.043
15° (0.966)	0.0385	0.154	0.092	0.0027	0.037
5° (0.996)	0.0015	0.147	0.089	0.000092	0.037

- Global maximum of $w_1(Q_1, Q_2, t) = 4.563$
  ($Q_1 = 0.177$ GeV, $Q_2 = 0.145$ GeV, $\theta = 118.1°$ ($t = -0.471$))
- Global minimum of $w_1(Q_1, Q_2, t) = -0.0044$
  ($Q_1 = 0.118$ GeV, $Q_2 = 1.207$ GeV, $\theta = 45.7°$ ($t = 0.698$))
- Global maximum of $w_2(Q_1, Q_2, t) = 0.495$
  ($Q_1 = Q_2 = 0.097$ GeV and $\theta = 133.1°$ ($t = -0.684$))

Locations of maxima of $w_{1,2}(Q_1, Q_2, t)$ for η (top) and η' (bottom)

θ ($t = \cos\theta$)	Max. w_1	Q_1 [GeV]	Q_2 [GeV]	Max. w_2	$Q_1 = Q_2$ [GeV]
175° (-0.996)	0.117	0.328	0.328	0.0061	0.143
165° (-0.966)	0.341	0.327	0.327	0.018	0.142
150° (-0.866)	0.616	0.325	0.323	0.032	0.137
135° (-0.707)	0.778	0.323	0.317	0.041	0.131
120° (-0.5)	0.809	0.322	0.308	0.044	0.123
105° (-0.259)	0.729	0.323	0.296	0.040	0.114
90° (0.0)	0.575	0.328	0.282	0.032	0.106
75° (0.259)	0.395	0.336	0.267	0.023	0.096
60° (0.5)	0.231	0.346	0.253	0.014	0.087
45° (0.707)	0.107	0.356	0.241	0.0063	0.077
30° (0.866)	0.034	0.363	0.231	0.0019	0.067
15° (0.966)	0.0044	0.367	0.225	0.00023	0.063
5° (0.996)	0.00017	0.368	0.224	8×10^{-6}	0.065
175° (-0.996)	0.049	0.434	0.434	0.0020	0.143
165° (-0.966)	0.142	0.432	0.433	0.0059	0.142
150° (-0.866)	0.255	0.427	0.430	0.011	0.139
135° (-0.707)	0.320	0.419	0.423	0.014	0.134
120° (-0.5)	0.330	0.413	0.412	0.015	0.128
105° (-0.259)	0.293	0.412	0.397	0.014	0.120
90° (0.0)	0.227	0.418	0.378	0.011	0.112
75° (0.259)	0.154	0.431	0.358	0.0079	0.102
60° (0.5)	0.088	0.451	0.340	0.0047	0.092
45° (0.707)	0.041	0.472	0.326	0.0022	0.082
30° (0.866)	0.013	0.491	0.315	0.00066	0.072
15° (0.966)	0.0017	0.504	0.309	0.000079	0.067
5° (0.996)	0.000062	0.508	0.307	3×10^{-6}	0.070

Form factor $\mathcal{F}_{\pi^0\gamma^*\gamma^*}(q_1^2, q_2^2)$ and transition form factor $F(Q^2)$

- Form factor $\mathcal{F}_{\pi^0\gamma^*\gamma^*}(q_1^2, q_2^2)$ between an on-shell pion and two off-shell (virtual) photons:

$$i \int d^4x\, e^{iq_1\cdot x} \langle 0|\, T\{j_\mu(x) j_\nu(0)\} |\pi^0(q_1+q_2)\rangle = \varepsilon_{\mu\nu\alpha\beta}\, q_1^\alpha\, q_2^\beta\, \mathcal{F}_{\pi^0\gamma^*\gamma^*}(q_1^2, q_2^2)$$

$$j_\mu(x) = (\overline{\psi}\hat{Q}\gamma_\mu\psi)(x), \quad \psi \equiv \begin{pmatrix} u \\ d \\ s \end{pmatrix}, \quad \hat{Q} = \mathrm{diag}(2,-1,-1)/3$$

(light quark part of electromagnetic current)

Bose symmetry: $\mathcal{F}_{\pi^0\gamma^*\gamma^*}(q_1^2, q_2^2) = \mathcal{F}_{\pi^0\gamma^*\gamma^*}(q_2^2, q_1^2)$

Form factor for real photons is related to $\pi^0 \to \gamma\gamma$ decay width:

$$\mathcal{F}^2_{\pi^0\gamma^*\gamma^*}(q_1^2 = 0, q_2^2 = 0) = \frac{4}{\pi\alpha^2 m_\pi^3}\Gamma_{\pi^0\to\gamma\gamma}$$

Often normalization with chiral anomaly is used:

$$\mathcal{F}_{\pi^0\gamma^*\gamma^*}(0,0) = -\frac{1}{4\pi^2 F_\pi}$$

- Pion-photon transition form factor:

$$F(Q^2) \equiv \mathcal{F}_{\pi^0\gamma^*\gamma^*}(-Q^2, q_2^2 = 0), \qquad Q^2 \equiv -q_1^2$$

Note that $q_2^2 = 0$, but $\vec{q}_2 \neq \vec{0}$ for on-shell photon !

Form factor model: LMD+V (large-N_c QCD) versus VMD

For single-virtual FF, both models give equally good fit to CLEO data. Main difference: double-virtual case. VMD FF violates OPE, falls off too fast. For large Q^2:

$\mathcal{F}^{\mathrm{LMD+V}}_{\pi^0\gamma^*\gamma^*}(-Q^2,-Q^2) \sim \mathcal{F}^{\mathrm{OPE}}_{\pi^0\gamma^*\gamma^*}(-Q^2,-Q^2) \sim 1/Q^2$ versus $\mathcal{F}^{\mathrm{VMD}}_{\pi^0\gamma^*\gamma^*}(-Q^2,-Q^2) \sim 1/Q^4$

Define: $\Delta\mathcal{F}(Q_1^2,Q_2^2) = \mathcal{F}^{\mathrm{LMD+V}}_{\pi^0\gamma^*\gamma^*}(-Q_1^2,-Q_2^2) - \mathcal{F}^{\mathrm{VMD}}_{\pi^0\gamma^*\gamma^*}(-Q_1^2,-Q_2^2)$

$\dfrac{\mathcal{F}^{\mathrm{LMD+V}}_{\pi^0\gamma^*\gamma^*}(-Q_1^2,-Q_2^2)}{\mathcal{F}_{\pi^0\gamma^*\gamma^*}(0,0)}$

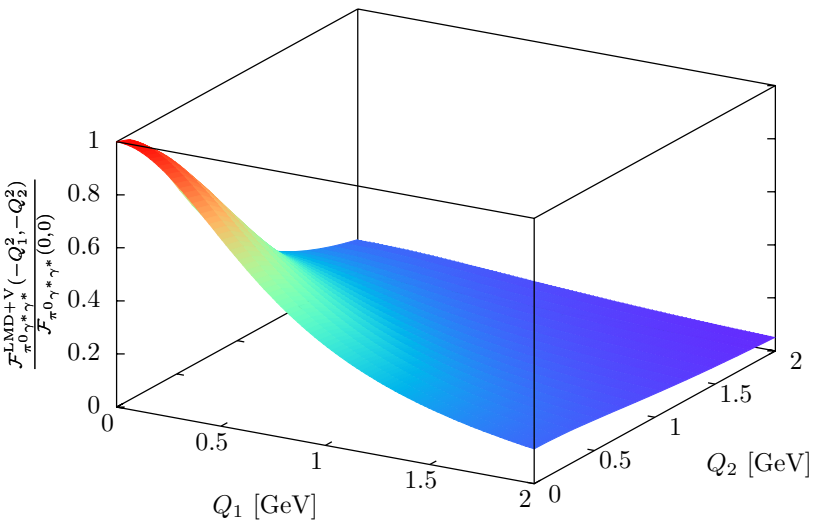

$\dfrac{\Delta\mathcal{F}(Q_1^2,Q_2^2)}{\mathcal{F}^{\mathrm{LMD+V}}_{\pi^0\gamma^*\gamma^*}(-Q_1^2,-Q_2^2)}$

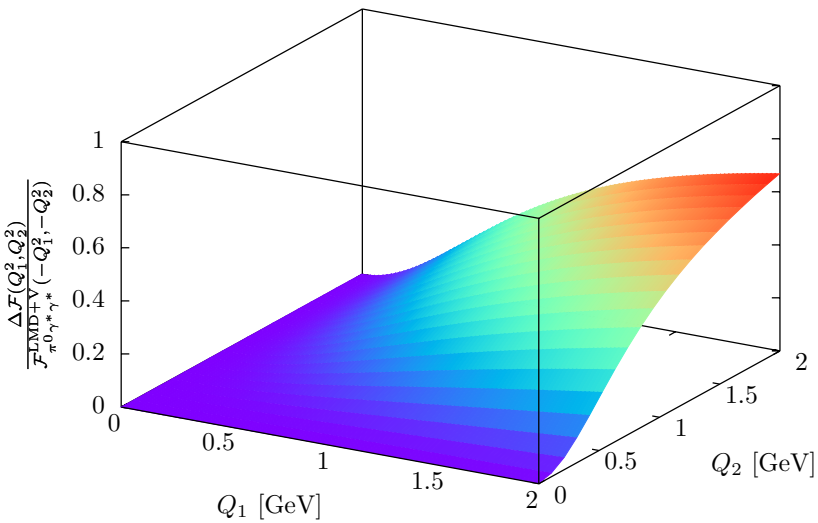

Q_1 [GeV]	Q_2 [GeV]	$\dfrac{\mathcal{F}^{\mathrm{LMD+V}}_{\pi^0\gamma^*\gamma^*}(-Q_1^2,-Q_2^2)}{\mathcal{F}_{\pi^0\gamma^*\gamma^*}(0,0)}$	$\dfrac{\mathcal{F}^{\mathrm{VMD}}_{\pi^0\gamma^*\gamma^*}(-Q_1^2,-Q_2^2)}{\mathcal{F}_{\pi^0\gamma^*\gamma^*}(0,0)}$	$\dfrac{\Delta\mathcal{F}(Q_1^2,Q_2^2)}{\mathcal{F}^{\mathrm{LMD+V}}_{\pi^0\gamma^*\gamma^*}(-Q_1^2,-Q_2^2)}$
0.5	0	0.707	0.706	0.0003
1	0	0.376	0.376	0.001
0.5	0.5	0.513	0.499	0.027
1	1	0.183	0.141	0.23

Since LMD+V and VMD FF differ for $Q_1 = Q_2 = 1$ GeV by 23%, it might be possible to distinguish the two models experimentally at BES III, if binning is chosen properly.

The LMD+V form factor

Knecht, AN, EPJC '01; AN '09

- Ansatz for $\langle VVP \rangle$ and thus $\mathcal{F}_{\pi^0\gamma^*\gamma^*}$ in large-N_c QCD in chiral limit with 1 multiplet of lightest pseudoscalars (Goldstone bosons) and 2 multiplets of vector resonances, ρ, ρ' (lowest meson dominance (LMD) + V).
- $\mathcal{F}_{\pi^0\gamma^*\gamma^*}$ fulfills all leading and some subleading QCD short-distance constraints from operator product expansion (OPE).
- Reproduces Brodsky-Lepage (BL): $\lim\limits_{Q^2\to\infty} \mathcal{F}_{\pi^0\gamma^*\gamma^*}(-Q^2,0) \sim 1/Q^2$

  (OPE and BL cannot be fulfilled simultaneously with only one vector resonance).
- Normalized to decay width $\Gamma_{\pi^0\to\gamma\gamma}$

$$\mathcal{F}^{\mathrm{LMD+V}}_{\pi^0\gamma^*\gamma^*}(q_1^2,q_2^2) = \frac{F_\pi}{3}\,\frac{q_1^2\,q_2^2\,(q_1^2+q_2^2)+h_1\,(q_1^2+q_2^2)^2+\bar{h}_2\,q_1^2\,q_2^2+\bar{h}_5\,(q_1^2+q_2^2)+\bar{h}_7}{(q_1^2-M_{V_1}^2)\,(q_1^2-M_{V_2}^2)\,(q_2^2-M_{V_1}^2)\,(q_2^2-M_{V_2}^2)}$$

$F_\pi = 92.4$ MeV, $M_{V_1} = M_\rho = 775.49$ MeV, $M_{V_2} = M_{\rho'} = 1.465$ GeV

Free model parameters: $h_i, \bar{h}_i$

Transition form factor:

$$F^{\mathrm{LMD+V}}(Q^2) = \frac{F_\pi}{3}\,\frac{1}{M_{V_1}^2\,M_{V_2}^2}\,\frac{h_1\,Q^4-\bar{h}_5\,Q^2+\bar{h}_7}{(Q^2+M_{V_1}^2)(Q^2+M_{V_2}^2)}$$

- $h_1 = 0$ GeV^2 (Brodsky-Lepage behavior $\mathcal{F}^{\mathrm{LMD+V}}_{\pi^0\gamma^*\gamma}(-Q^2,0) \sim 1/Q^2$)
- $\bar{h}_2 = -10.63$ GeV^2 (Melnikov, Vainshtein '04: Higher twist corrections in OPE)
- $\bar{h}_5 = 6.93 \pm 0.26$ GeV$^4 - h_3 m_\pi^2$ (fit to CLEO data of $\mathcal{F}^{\mathrm{LMD+V}}_{\pi^0\gamma^*\gamma}(-Q^2,0)$)
- $\bar{h}_7 = -\frac{N_c M_{V_1}^4 M_{V_2}^4}{4\pi^2 F_\pi^2} = -14.83$ GeV^6 (or normalization to $\Gamma(\pi^0\to\gamma\gamma)$)

The VMD form factor

Vector Meson Dominance:

$$\mathcal{F}^{\mathrm{VMD}}_{\pi^{0*}\gamma^*\gamma^*}(q_1^2, q_2^2) = -\frac{N_c}{12\pi^2 F_\pi} \frac{M_V^2}{q_1^2 - M_V^2} \frac{M_V^2}{q_2^2 - M_V^2}$$

Only two model parameters: F_π and M_V

Note:

- VMD form factor factorizes $\mathcal{F}^{\mathrm{VMD}}_{\pi^0\gamma^*\gamma^*}(q_1^2, q_2^2) = f(q_1^2) \times f(q_2^2)$. This might be a too simplifying assumption / representation.
- VMD form factor has wrong short-distance behavior: $\mathcal{F}^{\mathrm{VMD}}_{\pi^0\gamma^*\gamma^*}(q^2, q^2) \sim 1/q^4$, for large q^2, falls off too fast compared to OPE prediction $\mathcal{F}^{\mathrm{OPE}}_{\pi^0\gamma^*\gamma^*}(q^2, q^2) \sim 1/q^2$.

Transition form factor:

$$F^{\mathrm{VMD}}(Q^2) = -\frac{N_c}{12\pi^2 F_\pi} \frac{M_V^2}{Q^2 + M_V^2}$$